

A Bayesian Classification Trees Approach to Treatment Effect Variation with Noncompliance

Jared D. Fisher, David W. Puelz, Sameer K. Deshpande

August 28, 2024

Abstract

Estimating varying treatment effects in randomized trials with noncompliance is inherently challenging since variation comes from two separate sources: variation in the impact itself and variation in the compliance rate. In this setting, existing flexible machine learning methods are highly sensitive to the weak instruments problem, in which the compliance rate is (locally) close to zero. Our main methodological contribution is to present a Bayesian Causal Forest model for binary response variables in scenarios with noncompliance. By repeatedly imputing individuals' compliance types, we can flexibly estimate heterogeneous treatment effects among compliers. Simulation studies demonstrate the usefulness of our approach when compliance and treatment effects are heterogeneous. We apply the method to detect and analyze heterogeneity in the treatment effects in the Illinois Workplace Wellness Study, which not only features heterogeneous and one-sided compliance but also several binary outcomes of interest. We demonstrate the methodology on three outcomes one year after intervention. We confirm a null effect on the presence of a chronic condition, discover meaningful heterogeneity impact of the intervention on metabolic parameters though the average effect is null in classical partial effect estimates, and find substantial heterogeneity in individuals' perception of management prioritization of health and safety.

arXiv:2408.07765v2 [stat.AP] 26 Aug 2024

1 Introduction

1.1 The effectiveness of workplace wellness programs

Many employers pay their employees to adopt and maintain healthy habits like regular exercise, dieting, or other wellness practices. This pay often comes in the form of rebates of healthcare premiums or compensation in addition to salary. From an employer’s perspective, healthier employees may be more productive, be happier in their jobs, and incur fewer healthcare costs. On this view, workplace wellness programs offer potentially high return on investment, benefiting both employer and employees.

To examine the practical effects of workplace wellness programs, a randomized controlled trial was conducted at the University of Illinois at Urbana-Champaign (Jones et al., 2019; Reif et al., 2020). A workplace wellness program, called iThrive, was offered to the treatment group while a control group was also monitored. 12,459 benefits-eligible employees were invited to be part of the study, with 4,834 joining the study. 3,300 of these were randomly assigned to the treatment group and invited to participate in iThrive. Financial awards were given for participating in the program, though not all invitees actually participated. The other 1,534 subjects were not invited to the program and thus comprise the control group. Jones et al. (2019) found that iThrive had no significant effect on 40 out of 42 outcomes related to healthcare spending, job productivity, and health behaviors measured 12 and 24 months after the start of iThrive. Participation in iThrive did, however, significantly increase the likelihood that participants received a health screening and believed that their managers prioritized employee health and safety. Reif et al. (2020) extended Jones et al. (2019)’s analysis, finding that iThrive had an insignificant effect on several biometric outcomes, diabetes, hypertension, and hospital visits with two exceptions: participants were more likely to have a primary care physician and to have positive beliefs about their own health. In this paper, we examine the extent to which the apparent null effects are a product of offsetting positive and negative effects within subgroups of the study population. That is, we examine the potential heterogeneity of iThrive’s effect on health outcomes.

1.2 Noncompliance and treatment effect heterogeneity

Randomized controlled trials with noncompliance exist somewhere between observational studies and randomized experiments. The intervention is indeed randomly assigned but is imperfectly taken by the subjects. Two common approaches to deal with noncompliance are instrumental variable techniques and principal stratification. For trials with noncompliance, the random assignment acts as the instrument if it is only correlated with outcomes through the actual receipt of treatment. Principal stratification refers to identifying different subgroups of interest based on post-randomization variables, such as the actual receipt of treatment. Formalized by Frangakis and Rubin (2002), these subgroups, called principal strata, can have different treatment effects; see Page et al. (2015) for an overview of methods for estimating these subgroup effects.

Treatment effect heterogeneity can also complicate the detection of population treatment effects. It could be the case that some subjects have a positive treatment effect, while other have an opposite, negative treatment effect, resulting in a null population average effect. These two halves of the population likely differ in important ways, and the variables that describe differences in effects are called moderators. When the moderators are not known *a priori*, they must be discovered while estimating the treatment effect heterogeneity. In recent years, tree-based machine learning methods have emerged as popular and effective approaches for this task. Three, in particular, stand out. Hill (2011) proposed a two-step process: first one uses Bayesian additive regression trees (BART; Chipman et al., 2010) to estimate the conditional expectation of the outcome given treatment and covariates; and second, one estimates causal effects with differences in evaluations of the estimated conditional expectation function. Hahn et al. (2020) argued that their Bayesian causal forests (BCF) model, which jointly estimates the prognostic function and treatment effect function with separate BART ensembles, provides more transparent, targeted, and effective regularization of the treatment effects. Finally, Wager and Athey (2018) introduced a random forests-based estimator (see also Athey and Wager, 2019).

1.3 Our contributions

We propose a BCF-based approach for estimating heterogeneous effects of a binary treatment on binary outcomes from randomized trials with one-sided noncompliance. Our work adds to a growing literature on heterogeneous effect estimation with instruments, principal stratification, and/or non-compliance. This literature includes [Athey et al. \(2019\)](#), which presents a random forests-based IV estimator in §7. [Johnson et al. \(2022\)](#) first identifies potential effect modifiers with interpretable machine learning methods and then tests for modifier’s effect on the outcome with matching. [McCulloch et al. \(2021\)](#) and [Bargagli-Stoffi et al. \(2022\)](#) both present BART-based extensions of the popular two-stages least squares approach for IV regression. Before proceeding, we pause to highlight three recent works that also jointly estimate latent principal strata and treatment effects with BART. [Chen et al. \(2024\)](#) jointly model latent survival class with nested probit BART models and a continuous outcome using BART. [Kim and Zigler \(2024\)](#) jointly model a continuous intermediate variable and a continuous outcome variable with BCF-like models. [Garraza et al. \(2024\)](#) jointly model compliance strata with nested probit BART models and a binary outcome also using probit BART models. Whereas this last work separately estimates effects within each principal strata separately, we “borrow strength” across the strata.

In this paper, we jointly model the binary outcome and compliance status of all subjects in the iThrive study. Across several synthetic datasets, our joint modeling approach produced more accurate conditional local average treatment effects than methods that use a localized Wald estimator ([Wald, 1940](#)), which is a ratio of the conditional intention-to-treat effect on the outcome to that of the treatment receipt.

We found that subjects in the Illinois Workplace Wellness Study who (i) complied with the invitation to participate in the workplace wellness program and (ii) did not self-report high blood pressure, cholesterol, or blood glucose in 2016 were much more likely to self-report high values of these measures in 2017 than those who did not self-report high values in 2016. This suggests that participation in the programs made compliant subjects more aware of their own health conditions. We also found substantial heterogeneity in the effect of the program on employees’ view about management’s health and safety priorities.

This paper proceeds as follows. In [Section 2](#), we carefully define the causal estimand of interest and state the necessary assumptions needed to identify it from the observed data. We then present our estimation strategy in [Section 3](#). We report the results of several simulation studies that compare our proposed approach to existing methods in [Section 4](#). In [Section 5](#), we re-analyze the data from the Illinois Workplace Wellness Study. We conclude in [Section 6](#) with a discussion of the strengths and limitations of our re-analysis and outline several methodological extensions.

2 Identification, heterogeneity, & non-compliance

For each subject $i = 1, \dots, n$, we observe (i) a p -dimensional covariate vector \mathbf{x}_i ; (ii) a binary indicator A_i recording whether they were invited to participate in the workplace wellness program ($A_i = 1$) or not ($A_i = 0$); (iii) a binary indicator $R_i^{\text{obs}} \in \{0, 1\}$ recording whether they actually participated in the program or not; and (iv) a binary outcome $Y_i^{\text{obs}} \in \{0, 1\}$. We wish to estimate the effect of participating in the workplace wellness program on several binary health outcomes varies with respect to \mathbf{x} . In doing so, we hope to identify who benefits the most from workplace wellness programs and by how much.

Momentarily leaving aside issues of heterogeneity, to determine whether workplace wellness programs have a constant effect on health outcomes, we could naively compare the average responses amongst the treated and control subjects:

$$\frac{\sum_i Y_i^{\text{obs}} \times \mathbb{1}(A_i = 1)}{\sum_i \mathbb{1}(A_i = 1)} - \frac{\sum_i Y_i^{\text{obs}} \times \mathbb{1}(A_i = 0)}{\sum_i \mathbb{1}(A_i = 0)}. \quad (1)$$

Although the comparison is unconfounded due to the random treatment assignment, it can be misleading because not every subject assigned to treatment actually receives it. In particular, if the workplace wellness program improved health outcomes, then the presence of non-compliers in the treatment arm may deflate

the effect estimated by Equation (1). To overcome this bias, it is tempting to compare the average response amongst treated subjects who actually received treatment to the average response amongst the control group:

$$\frac{\sum_i Y_i^{\text{obs}} \times \mathbb{1}(A_i = 1 \ \& \ R_i^{\text{obs}} = 1)}{\sum_i \mathbb{1}(A_i = 1 \ \& \ R_i = 1)} - \frac{\sum_i Y_i^{\text{obs}} \times \mathbb{1}(A_i = 0)}{\sum_i \mathbb{1}(A_i = 0)}. \quad (2)$$

Though intuitive, the estimator in Equation (2) remains unsatisfying in face of non-compliance, as it implicitly assumes that all control subjects would have participated in the wellness program had they been invited. Instead, the ideal comparison is between (i) treated subjects who received treatment and (ii) control subjects who would have received treatment had they been assigned treatment. Unfortunately, we cannot directly carry out the ideal comparison, as it involves reasoning about counterfactual outcomes that would have been observed under a potentially different received treatment.

In Section 2.1, we introduce several assumptions under which we can identify a constant local average treatment effect (LATE) in terms of the observed data $(A_i, R_i^{\text{obs}}, Y_i^{\text{obs}})$ and estimate it with the typical Wald estimator (Wald, 1940). Then, in Section 2.2, we turn our attention to the conditional local average treatment effect (LATE(\mathbf{x}) or CLATE) and argue that the natural extension of the Wald estimator can exhibit particularly pathological behavior in the presence of heterogeneous non-compliance.

2.1 Identifying & estimating a constant LATE

For each subject i , let $R_i(1)$ and $R_i(0)$ denote two potential binary “received treatments” under each treatment assignment. Using the terminology from Angrist et al. (1996), we can stratify our study population into four groups based on the value of $\{R_i(0), R_i(1)\}$: (i) never-takers $\{0, 0\}$; (ii) compliers $\{0, 1\}$; (iii) defiers $\{1, 0\}$; and (iv) always-takers $\{1, 1\}$. In the workplace wellness study, subjects were not able to participate in iThrive without an invitation. Thus, for every subject i , we have $R_i(0) = 0$, which implies that there are only never-takers and compliers in our study. We introduce the binary indicator C_i , which encodes whether subject i is a complier ($C_i = 1$) or a never-taker ($C_i = 0$). Note that this means that $C_i = R_i(1)$ and that $R_i(0)$ provides no information about subject i ’s compliance status. Finally, for each combination of assigned and potential received treatment $(A_i, R_i(A_i))$, we can define a potential outcome $Y_i(A_i, R_i(A_i))$ to be the outcome observed if a subject was assigned treatment A_i and received treatment $R_i(A_i)$. Each subject in our study has three potential outcomes: (i) the outcome that would be observed if they were invited to participate and did participate in the workplace wellness program $Y_i(1, 1)$; (ii) the outcome if they were invited to participate but ultimately did not participate $Y_i(1, 0)$; and (iii) the outcome if they were not invited to participate $Y_i(0, 0)$. Implicit in our notation is the standard “stable unit treatment value assumption” (SUTVA; hereafter assumption A1). Assumption A2 encodes our one-sided non-compliance assumption.

A1 (SUTVA): Potential outcomes do not vary with treatments assigned to other subjects and, for each subject, there are no different forms or versions of each treatment level, which lead to different treatment outcomes (Imbens and Rubin, 2015).

A2 (One-sided Noncompliance): for all subjects i , $R_i(0) = 0$.

Assumption A2 is stronger than the “no defiers”/monotonicity assumption that is traditionally assumed many principal stratification settings (§24.5.2 Imbens and Rubin, 2015) as it also does not allow for always-takers. The (constant) local average treatment effect is $\text{LATE} = \mathbb{E}[Y_i(1, 1) - Y_i(0, 0) | C_i = 1]$. In order to identify the constant LATE, we make several standard assumptions that apply for all subjects i .

A3 (Exclusion Restriction): Assignment to treatment has no effect on the outcome except through the receipt of treatment: $Y_i(0, 0) = Y_i(1, 0)$.

A4 (Unconfoundedness): Potential outcomes and received treatments are independent of assigned treatment: $A_i \perp [R_i(0), R_i(1), Y_i(0, 0), Y_i(1, 0), Y_i(1, 1)]$.

A5 (Existence of Compliers): $0 < \mathbb{P}(C_i = 1)$.

A6 (Overlap): $0 < \mathbb{P}(A_i = 1) < 1$.

Assumption **A3** encodes the belief that assignment to treatment affects the outcome only through the actual receipt of treatment. Assumption **A4** is usually satisfied by random treatment assignment. Assumptions **A5** and **A6** allow estimation to be meaningful, as there are at least some compliers and some units assigned to each treatment arm.

Under Assumptions **A1–A6**, we could identify LATE as

$$\text{LATE} = \mathbb{E}[Y_i^{\text{obs}} | C_i = 1, A_i = 1] - \mathbb{E}[Y_i^{\text{obs}} | C_i = 1, A_i = 0] \quad (3)$$

if we could observe the compliance status of all subjects. Equation (3) suggests a natural estimator: simply compare the average outcomes amongst compliers in each treatment arm. Unfortunately, we only observe $\mathbf{C}^{(1)} = \{C_i : A_i = 1\}$ and do not observe $\mathbf{C}^{(0)} = \{C_i : A_i = 0\}$, rendering that estimator infeasible.

To overcome this difficulty, it is common in the instrumental variables literature to estimate LATE with the Wald estimator (Wald, 1940), defined as the ratio of two “intention-to-treat” (ITT) estimates. To motivate such estimators, first observe that under Assumption **A1** we can identify ITT_R , and under Assumptions **A1** and **A4** (see Appendix A), we can identify the ITT_Y :

$$\begin{aligned} \text{ITT}_R &:= \mathbb{E}[R_i(1) - R_i(0)] = \mathbb{E}[R_i^{\text{obs}} | A_i = 1] - \mathbb{E}[R_i^{\text{obs}} | A_i = 0] \\ \text{ITT}_Y &:= \mathbb{E}[Y_i(1, R_i(1)) - Y_i(0, R_i(0))] = \mathbb{E}[Y_i^{\text{obs}} | A_i = 1] - \mathbb{E}[Y_i^{\text{obs}} | A_i = 0]. \end{aligned} \quad (4)$$

Assumptions **A1–A3** and **A5** allow us to write $\text{LATE} = \text{ITT}_Y / \text{ITT}_R$, which provides the same estimator as a two-stage least squares IV regression with no covariates (§4.1.2 Angrist and Pischke, 2009). Thus, by Assumption **A2** and the fact that $Y_i^{\text{obs}}, R_i^{\text{obs}} \in \{0, 1\}$,

$$\text{LATE} = \frac{\mathbb{P}(Y_i^{\text{obs}} = 1 | A_i = 1) - \mathbb{P}(Y_i^{\text{obs}} = 1 | A_i = 0)}{\mathbb{P}(R_i^{\text{obs}} = 1 | A_i = 1)}. \quad (5)$$

2.2 The *conditional* local average treatment effect

Up to this point, our discussion has focused on estimating a constant effect. In reality, we believe it more likely that the workplace wellness program will benefit only some subjects. Further, we believe that not all subjects are equally likely to be compliers. To probe potential heterogeneity, we focus on a natural analog of LATE, the *conditional* local average treatment effect (CLATE): $\text{LATE}(\mathbf{x}) = \mathbb{E}[Y_i(1, 1) - Y_i(0, 0) | C_i = 1, \mathbf{X}_i = \mathbf{x}]$. To identify $\text{LATE}(\mathbf{x})$, we replace Assumption **A4–A6** with their *conditional* versions.

Ax4 (Unconfoundedness): Given \mathbf{x} , potential outcomes and received treatments are independent of assigned treatment: $A_i \perp [R_i(0), R_i(1), Y_i(0, 0), Y_i(1, 0), Y_i(1, 1)] | \mathbf{X}_i = \mathbf{x}$.

Ax5 (Existence of Compliers): $0 < \mathbb{P}(C_i = 1 | \mathbf{X}_i = \mathbf{x})$.

Ax6 (Overlap): $0 < \mathbb{P}(A_i = 1 | \mathbf{X}_i = \mathbf{x}) < 1$.

Under these assumptions, we would ideally estimate

$$\text{LATE}(\mathbf{x}) = \mathbb{E}[Y_i^{\text{obs}} | C_i = 1, A_i = 1, \mathbf{X}_i = \mathbf{x}] - \mathbb{E}[Y_i^{\text{obs}} | C_i = 1, A_i = 0, \mathbf{X}_i = \mathbf{x}]. \quad (6)$$

Because we do not fully observe $\mathbf{C} = \mathbf{C}^{(0)} \cup \mathbf{C}^{(1)}$, we cannot operationalize Equation (6), by, for instance, regressing Y_i^{obs} onto A_i and \mathbf{X}_i using data from the compliers. Under Assumptions **A1–A3** and Assumptions **Ax4–Ax6**, a natural extension of the ratio estimator in Equation (5) is

$$\text{LATE}(\mathbf{x}) = \frac{\mathbb{P}(Y_i^{\text{obs}} = 1 | A_i = 1, \mathbf{X}_i = \mathbf{x}) - \mathbb{P}(Y_i^{\text{obs}} = 1 | A_i = 0, \mathbf{X}_i = \mathbf{x})}{\mathbb{P}(R_i^{\text{obs}} = 1 | A_i = 1, \mathbf{X}_i = \mathbf{x})}. \quad (7)$$

There are many ways to implement the estimator in Equation (7) by separately modeling the numerator and denominator. To estimate the numerator, we could use any number of causal machine learning approaches, e.g., Hill (2011), Künzel et al. (2019), Athey et al. (2019), Hahn et al. (2020). Regardless of how we estimate the numerator, however, the estimator in Equation (7) becomes extremely unstable whenever $\mathbb{P}(R_i^{\text{obs}} = 1 | A_i = 1, \mathbf{X}_i = \mathbf{x})$ is near zero. So, estimating $\text{LATE}(\mathbf{x})$ for individuals who are unlikely to be compliers can be fraught. This situation is termed the “weak instrument problem.”

2.3 The weak instrument problem and the local compliance rate

In instrumental variables analyses, an important consideration is the relevance of the instrument, i.e. the strength of the instrument’s relationship with the treatment. For us, the instrument is the assignment to treatment A_i and the treatment is $R_i(A_i)$. If A_i has no causal effect on $R_i(A_i)$, then clearly $\text{ITT}_R = \mathbb{E}[R_i(1) - R_i(0)] = 0$ and the Wald estimator is undefined. Under the aforementioned assumptions, as $R_i(1) = C_i$ and $R_i(0) = 0$, we see that this denominator is equivalent to the compliance rate $\mathbb{P}(C_i = 1)$.

The weak instrument problem is well known (Andrews et al., 2019), and a compliance rate near zero would be an obvious indicator of a challenged experiment. However, as we move from estimating global LATE to the conditional $\text{LATE}(\mathbf{x})$, and specifically move from Assumption A5 to Assumption Ax5, we have another consideration: heterogeneity in compliance rate may mean that, while the global compliance rate is reasonable, the local compliance rate near certain values of \mathbf{X} may present a locally weak instrument. In Section 3, we propose an alternative that does not use the standard Wald estimator but instead models compliance, akin to Ratkovic and Shiraito (2014) and Imbens and Rubin (2015). Later we examine, via simulation, what happens when heterogeneous compliance rates yield locally weak instruments in Section 4.1.

3 Estimating the CLATE with BART

We essentially must estimate the response surface $\mathbb{P}(Y_i^{\text{obs}} = 1 | C_i = c, A_i = a, \mathbf{X}_i = \mathbf{x})$ *without observing \mathcal{C} , the full set of compliance statuses*. To this end, we specify a *joint* model for (Y^{obs}, C) that will allow us to (i) impute the missing compliance statuses $\mathbf{C}^{(0)}$ and then (ii) conditionally estimate the needed response surface. Specifically, we model

$$\begin{aligned} \mathbb{P}(Y_i = 1 | C_i = c_i, A_i = a_i, \mathbf{X}_i = \mathbf{x}_i) &= \Phi [\mu(\mathbf{x}_i) + c_i \times \mu_c(\mathbf{x}_i) + c_i \times a_i \times \tau(\mathbf{x}_i)] \\ \mathbb{P}(C_i = 1 | \mathbf{X}_i = \mathbf{x}_i) &= \Phi [\eta(\mathbf{x}_i)]. \end{aligned} \tag{8}$$

We approximate each of μ , μ_c , τ , and η with a regression tree ensemble and compute a joint posterior distribution over the missing compliance statuses and the tree ensembles. Since the posterior distribution is analytically intractable, we simulate draws from the posterior over regression tree ensembles using Markov chain Monte Carlo.

3.1 Prior regularization

Before specifying the prior and describing our posterior sampling strategy, we assume without loss of generality that all continuous covariates are re-scaled to the interval $[0,1]$ and introduce some additional notation. A regression tree (T, \mathcal{B}) is comprised of a binary decision tree T , which consists of collection of internal nodes and a collection of terminal or *leaf nodes*, and a collection \mathcal{B} of scalar *jumps*, one for each leaf. Each internal node of T is associated with a decision rule $\{X_j \in \mathcal{C}\}$. When X_r is continuous variable, \mathcal{C} is a half-open interval of the form $[0, c)$ and when X_j is categorical, \mathcal{C} is a subset of the possible levels of that variable. Given T , we can associate each \mathbf{x} with a single leaf by tracing a path down the tree by following the decision rules. Specifically, whenever the path encounters the rule $\{X_j \in \mathcal{C}\}$, it proceeds to the left (resp. right) if $x_j \in \mathcal{C}$ (resp. $x_j \notin \mathcal{C}$). This way, the decision tree T partitions the covariate space into disjoint regions, one for each leaf. Denoting the jump associated with leaf ℓ as β_ℓ , the pair (T, \mathcal{B}) , represents a piece-wise constant function that returns β_ℓ for all \mathbf{x} in the region associated with leaf ℓ .

For compactness, we use $\mathcal{E}^{(\mu)} = \{(T_m^\mu, \mathcal{B}_m^{(\mu)}) : m = 1, \dots, M^{(\mu)}\}$ to denote the ensemble of $M^{(\mu)}$ regression trees used to approximate μ . We similarly define $\mathcal{E}^{(\mu_c)}$, $\mathcal{E}^{(\tau)}$, and $\mathcal{E}^{(\eta)}$ for the remaining ensembles. Like [Hahn et al. \(2020\)](#) and [Deshpande et al. \(2024\)](#), we specify independent priors for each ensemble in \mathcal{E} and place independent and identical priors on the regression trees within each ensemble. For ease of exposition, we only describe the regression tree prior for $\mathcal{E}^{(\mu)}$ as the priors for the remaining ensembles are analogous. The regression tree prior consists of three parts: (i) a marginal prior over the structure of the decision tree; (ii) a conditional prior over the decision rules given the tree structure; and (iii) a condition prior for the jumps \mathcal{B} given the decision tree.

We can describe the tree structure prior with a branching process in which nodes are added sequentially so that whenever a new node is added at depth d , two children at depth $d+1$ are attached to it with probability $0.95(1+d)^{-2}$. This prior places overwhelming prior probability on trees of depth five or less.

Conditional on the tree structure, we sequentially draw decision rules at each non-terminal node in two steps. First, we draw the splitting variable index $j \sim \text{Multinomial}(\theta_1^{(\mu)}, \dots, \theta_p^{(\mu)})$. Then, conditional on j , we set \mathcal{C} to be a random subset of $\mathcal{A}(j)$, the set of available X_j values at the current non-terminal node. If X_j is continuous, we set $\mathcal{C} = [0, c]$ where c is drawn uniformly from the interval $\mathcal{A}(j)$. Otherwise, if X_j is categorical, we set \mathcal{C} to be a random non-trivial subset of the discrete set $\mathcal{A}(j)$. Following [Linero \(2018\)](#), we model $(\theta_1^{(\mu)}, \dots, \theta_p^{(\mu)}) \sim \text{Dirichlet}(\xi^{(\mu)}/p, \dots, \xi^{(\mu)}/p)$ and $\xi^{(\mu)}/(\xi^{(\mu)} + p) \sim \text{Beta}(0.5, 1)$.

Finally, conditional on the decision tree T , we respectively place independent normal priors with mean $\beta_0^{(\mu)}/M^{(\mu)}$ and variance $\sigma^2(\mu)/M^{(\mu)}$ on the jumps in \mathcal{B} , where $\beta_0^{(\mu)}$ and $\sigma^{(\mu)}$ are fixed constants. We specify similar priors for the other ensembles $\mathcal{E}^{(\mu_c)}$, $\mathcal{E}^{(\tau)}$, and $\mathcal{E}^{(\eta)}$. We recommend using 50 trees in each ensemble (i.e., setting $M^{(\mu)} = M^{(\mu_c)} = M^{(\tau)} = M^{(\eta)} = 50$) and the following hyper-parameter settings: $(\beta_0^{(\mu)}, \sigma^{(\mu)}) = (\Phi^{-1}(\bar{y}), 1.5)$; $(\beta_0^{(\eta)}, \sigma^{(\eta)}) = (\Phi^{-1}(\bar{c}), 1.5)$; $(\beta_0^{(\mu_c)}, \sigma^{(\mu_c)}) = (0, 0.5)$; and $(\beta_0^{(\tau)}, \sigma^{(\tau)}) = (0, 0.5)$ where \bar{y} is the average response in the whole dataset and \bar{c} is the observed compliance rate among treated subjects. These choices imply the following marginal priors: $\mu(\mathbf{x}) \sim \mathcal{N}(\Phi^{-1}(\bar{y}), 1.5^2)$; $\eta(\mathbf{x}) \sim \mathcal{N}(\Phi^{-1}(\bar{c}), 1.5^2)$; $\mu_c(\mathbf{x}) \sim \mathcal{N}(0, 0.5^2)$; and $\tau(\mathbf{x}) \sim \mathcal{N}(0, 0.5^2)$. In other words, we shrink each subjects' compliance and outcome probabilities towards the overall averages observed in the dataset. Bounding the CLATE with the first-order approximation

$$\text{LATE}(\mathbf{x}) \approx \tau(\mathbf{x}) \times \phi(\mu(\mathbf{x}) + c \times \mu_c(\mathbf{x})) \leq (2\pi)^{-1/2} |\tau(\mathbf{x})|,$$

we see that our prior places approximate 68% probability on the event that $|\text{LATE}(\mathbf{x})| < 0.2$. In the context of the workplace wellness studies, a 20-percentage point effect is quite large, making our prior on $\text{LATE}(\mathbf{x})$ fairly weakly informative.

3.2 Posterior computation

We use a Gibbs sampler to simulate draws from the joint posterior distribution $p(\mathbf{C}^{(0)}, \mathcal{E}, \Theta, \xi, \mathbf{Y}, \mathbf{C}^{(1)})$, where $\Theta = \{\theta^{(\mu)}, \theta^{(\mu_c)}, \theta^{(\tau)}, \theta^{(\eta)}\}$ is the collection of prior splitting probabilities for each ensemble and $\xi = \{\xi^{(\mu)}, \xi^{(\mu_c)}, \xi^{(\tau)}, \xi^{(\eta)}\}$ are the corresponding prior hyperparameters. We provide a high-level overview of the sampler here and present a detailed derivation in [Appendix B](#). Each iteration of our sampler involves four steps. In the first step, we draw the missing compliance statuses $\mathbf{C}^{(0)}$ conditionally given the ensembles \mathcal{E} and \mathbf{Y} . The missing C_i 's are conditionally independent of one another given \mathcal{E} and \mathbf{Y} (see [Equations \(B1\)](#) and [\(B2\)](#)).

After drawing the missing $\mathbf{C}^{(0)}$, we sequentially update each regression tree in \mathcal{E} in the second step of our sampler. To facilitate these updates, we introduce latent utilities \tilde{Y}_i and \tilde{C}_i such that $Y_i = \mathbb{1}(\tilde{Y}_i \geq 0)$ and $C_i = \mathbb{1}(\tilde{C}_i)$. Conditional on these latent utilities, we sweep over the trees in \mathcal{E} , updating them one at a time while holding the others fixed. Each individual tree update proceeds in two steps. First, we draw a new tree structure from its *marginal* distribution using a Metropolis-Hastings step in which proposals are

drawn by randomly growing or pruning the current tree structure. Then, we draw a new collection of jumps \mathcal{B} from its conditional distribution given the new tree structure and all other regression trees. Essentially, these tree updates turn out to be nothing more than a weighted version of [Chipman et al. \(2010\)](#)’s original Bayesian backfitting strategy that was also used in [Hahn et al. \(2020\)](#) and [Deshpande et al. \(2024\)](#). After updating each regression tree in \mathcal{E} , we sample new values of each vector in Θ conditionally on η using a conjugate Dirichlet-Multinomial update before drawing new values of η using an independence Metropolis step.

4 Simulations

We investigated the operating characteristics of our proposed approach (hereafter **BCF-LATE**) using three synthetic data simulation studies. We compared **BCF-LATE** with two versions of the Wald estimator (Equation (7)): **GRF**, the generalized random forest of [Athey et al. \(2019\)](#), and **Wald-BART**, which uses BART to estimate the expectations in the numerator and denominator of the Wald estimator. We specifically assessed how well each method could (i) predict $\text{LATE}(\mathbf{x}_i)$ for each simulated subject and (ii) quantify its uncertainty about those predictions. For each study, we generated n observations $(\mathbf{x}_1, A_1, R_1^{\text{obs}}, Y_1^{\text{obs}}), \dots, (\mathbf{x}_n, A_n, R_n^{\text{obs}}, Y_n^{\text{obs}})$ as follows. First, covariates $\mathbf{x}_i \in [-1, 1]^p$ are uniformly drawn. Then random treatment assignment A_i , treatment receipt R_i^{obs} , and outcome Y_i^{obs} are drawn as

$$\begin{aligned} A_i &\sim \text{Bernoulli}(0.5) & C_i &\sim \text{Bernoulli}(p_i^c) & p_i^c &= \Phi[\eta(\mathbf{x}_i)] \\ R_i^{\text{obs}} &= A_i C_i & Y_i^{\text{obs}} &\sim \text{Bernoulli}(p_i^y) & p_i^y &= \Phi[\mu(\mathbf{x}_i) + C_i \mu_c(\mathbf{x}_i) + A_i C_i \tau(\mathbf{x}_i)]. \end{aligned}$$

We used different functions μ , μ_c , τ , and η in each simulation study. When visualizing the results, variability/uncertainty is shown by shading 0.65, 1.3, and 2 standard errors for around the estimates from frequentist methods and, for Bayesian methods, shading the 50%, 80%, and 95% pointwise posterior credible intervals. Likewise, to show variability across simulations, we shade the 50%, 80%, and 95% intervals across simulation replications.

4.1 Visualizing the weak instrument problem

To visualize the differences between each method, we set $p = 1$ for our first simulation study. For this study, we drew each \mathbf{x}_i uniformly from $[-1, 1]$ and generated the data using

$$\eta(x) = 0 \quad \mu(x) = \sin(6x) \quad \mu_c(x) = -x \quad \tau(x) = 2 \times \mathbb{1}(x \leq 0) - 1.$$

The top row of Figure 4 shows each of $\mu(x)$, $\mu_c(x)$ and $\tau(x)$ with **BCF-LATE**’s posterior mean (solid line) and shaded regions for the pointwise posterior credible intervals. **BCF-LATE** recovers each of $\mu(x)$, $\mu_c(x)$, and $\tau(x)$ reasonably well; the 95% pointwise credible intervals for $\mu(x)$ and $\mu_c(x)$ had more than the nominal 95% frequentist coverage and the intervals for $\tau(x)$ covered about 88% of evaluations on average across 100 replications. Although $\tau(x)$ takes only two values, the function of interest, $\text{LATE}(x)$ is more complicated (bottom row of Figure 4). In this setting with a moderate, homogeneous compliance rate, all three methods performed similarly, with **BCF-LATE** enjoying a slight advantage. Across 100 simulation replications, the average root mean square errors (RMSE) for evaluating $\text{LATE}(x)$ were 0.105 (**BCF-LATE**), 0.110 (**Wald-BART**), and 0.114 (**GRF**) and the average coverage of the 95% uncertainty intervals were 86.9% (**BCF-LATE**), 97.4% (**Wald-BART**), and 86.1% (**GRF**). While **Wald-BART**’s coverage is much closer to the target 95%, we note that its intervals are much wider than the other methods’ intervals, as seen in Figure 4.

While it is reassuring that **BCF-LATE** performs well when all subjects have the same, moderately large compliance probability, the heterogeneous compliance setting is arguably more relevant. Recall from Section 2,

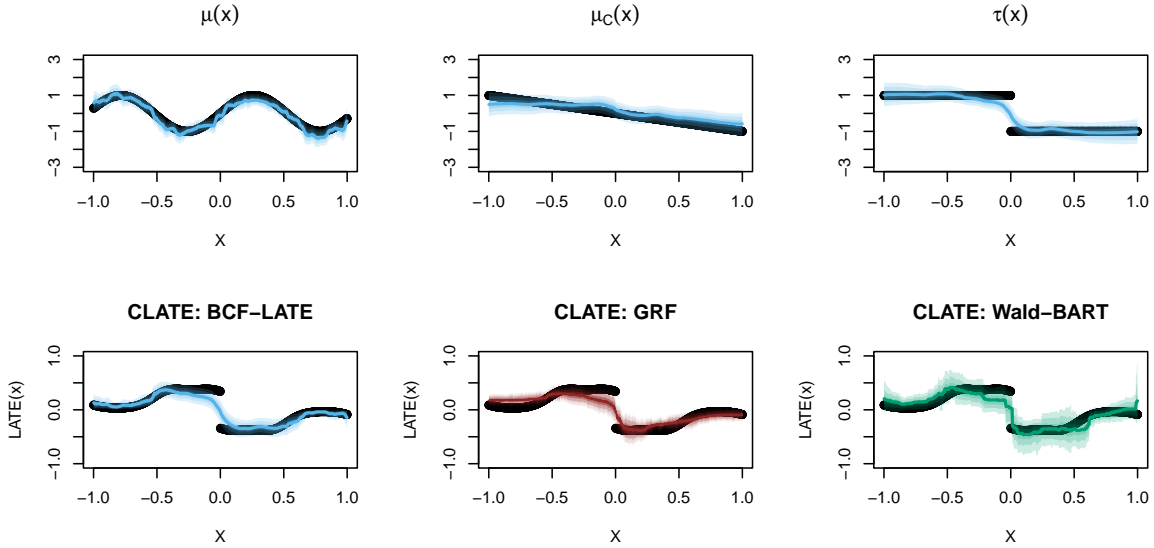


Figure 1: Comparison of different methods' estimation of heterogeneous CLATEs when a univariate data-generating process has a constant, large compliance rate.

that we observe three types of subjects, each with their own outcome model:

$$\mathbb{P}(Y_i = 1|C_i, A_i, \mathbf{X}_i = \mathbf{x}) = \begin{cases} \Phi[\mu(\mathbf{x})] & \text{if } C_i = 0 \\ \Phi[\mu(\mathbf{x}) + \mu_c(\mathbf{x})] & \text{if } C_i = 1 \text{ and } A_i = 0 \\ \Phi[\mu(\mathbf{x}) + \mu_c(\mathbf{x}) + \tau(\mathbf{x})] & \text{if } C_i = 1 \text{ and } A_i = 1. \end{cases} \quad (9)$$

Intuitively, we might expect to estimate $\mu(x)$ well when there is a large number of never-takers with $x_i \approx x$. Similarly, because there is no uncertainty about compliance status in the treatment arm, we would expect to estimate $\mu(x) + \mu_c(x) + \tau(x)$ well whenever there is a large number of invited compliers with $x_i \approx x$. So, if there are reasonably large sets of never-takers and invited compliers with $x_i \approx x$ we would expect BCF-LATE to also estimate their difference ($\mu_c(x) + \tau(x)$) well. To estimate LATE(x), however, we must disentangle $\mu_c(x)$ from $\tau(x)$. This is best done when the compliance rate when $\mathbb{P}(C_i = 1|x_i = x)$ is not too small and there are large numbers of compliers with $x_i \approx x$.

To check this intuition, we re-ran the simulation study using the same data generating functions as before but this time with $\eta(x) = -2x$. Figure 2 shows how BCF-LATE recovers each of $\mu(x)$, $\mu_c(x)$, $\tau(x)$, $\mathbb{P}(C = 1|x)$, $\mu_c(x) + \tau(x)$, and LATE(x). As anticipated, when x is small and the compliance rate is close to one (yielding few never-takers), the uncertainty bands of $\mu(x)$ widen in the top left pane. However, when there is a reasonable local sample size of never-takers (i.e., when the compliance rate is not close to 1), the function is well-estimated and the uncertainty intervals are tighter. Similarly, for values of more central values of x yielding non-extreme compliance probabilities, BCF-LATE produced shorter uncertainty intervals for $\mu_c(x) + \tau(x)$. For values of x closer to ± 1 , which produce extreme compliance probabilities, BCF-LATE returned much more uncertainty about this function. Turning to LATE(x), we find that BCF-LATE produced accurate estimates and well-calibrated uncertainty intervals.

Figure 3 compares BCF-LATE's ability to estimate LATE(x) in the presence of a weakening instrument with those of GRF and Wald-BART. As expected, all three methods do well when the compliance rate is large. However, as x increases and the compliance probability drops, we see that the uncertainty intervals for GRF and Wald-BART become much more erratic and inflated. Visually it further appears that BCF-LATE produced more accurate estimates of LATE(x), especially when the compliance probability was low. In fact, across

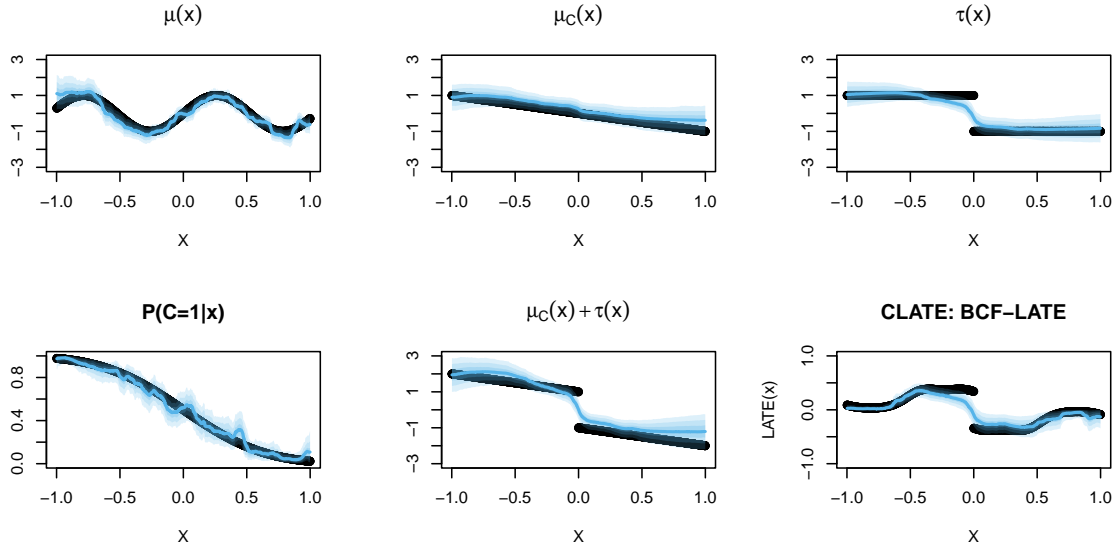


Figure 2: BCF-LATE fits for a univariate data-generating process with heterogeneous outcome and heterogeneous compliance.

100 simulation replications, BCFLATE’s average RMSE was 0.114, which was smaller than GRF’s (0.289) and Wald-BART’s (0.883).

4.2 Multiple covariates

Our second simulation study assessed how well BCF-LATE performs when n and p increase but when the underlying data-generating functions are relatively simple. For this study, for each combination of $n \in \{500, 2000, 5000\}$ and $p \in \{2, 5, 10, 25, 50, 75, 100\}$, we generated 100 datasets of size n using the functions

$$\eta(\mathbf{x}) = 4 \times \mathbb{1}(x_2 \geq 0.5) - 2 \quad \mu(\mathbf{x}) = \mu_c(\mathbf{x}) = 0 \quad \tau(\mathbf{x}) = 4 \times \mathbb{1}(x_1 \geq 0.5) - 2.$$

Figure 4a shows GRF’s RMSE (left) and interval score (IS, right) relative to BCF-LATE’s as a function of p with $n = 2000$ fixed. Figure 4b is analogous and shows how GRF’s relative RMSE and interval score changes

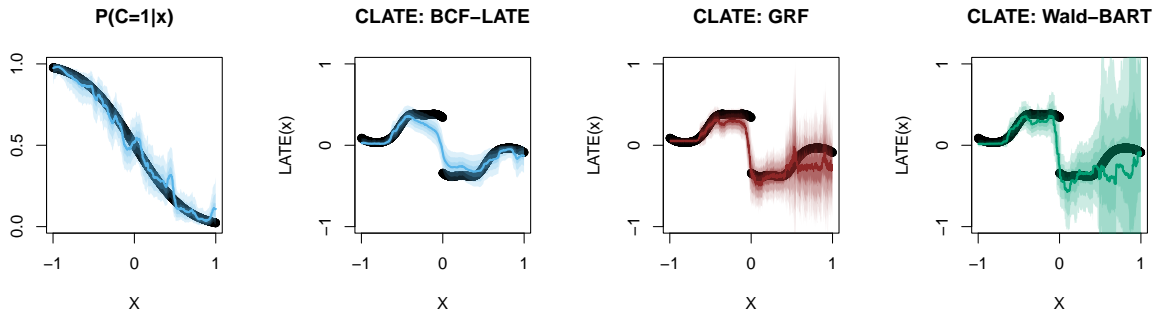


Figure 3: Comparison of different methods’ estimation of heterogeneous CLATEs from a univariate data-generating process. The compliance rate varies such that the instrument is weak when \mathbf{x} is large.

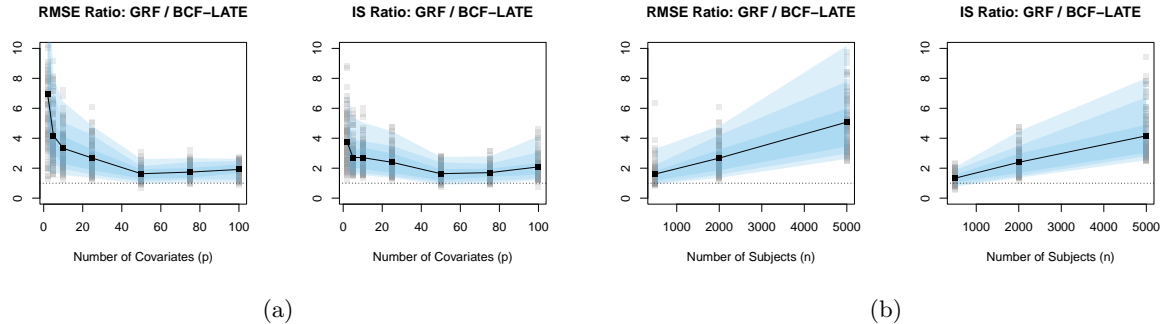


Figure 4: Comparison of BCF-LATE and GRF across 100 replications of the simple DGP when n is fixed and p increases (a) and when p is fixed and n increases (b). Each simulation is represented with a transparent gray square.

as n increased while fixing $p = 25$. The interval score combines interval coverage and interval width and is a proper scoring rule (Gneiting and Raftery, 2007). In the figures, values greater (resp. less) than one indicate that BCF-LATE performs better (resp. worse) than GRF. We see that for $n = 2000$ and small p , BCF-LATE is markedly better than GRF at estimating $\text{LATE}(\mathbf{x})$. While this performance gap shrinks as p increases, it does not go away: for $p = 5$, BCF-LATE’s RMSE is four times smaller than GRF’s and for $p = 100$, it is two times smaller. On further inspection, we found that as p increased, the width and coverage of BCF-LATE’s intervals increased while the width and coverage of GRF’s intervals decreased. Similarly, BCF-LATE’s edge in performance grows with the sample size n , for both point and interval estimation; see Tables C1 and C2 for a more detailed tabulation of the results.

4.3 Complicated Data Generating Process

In our third simulation study, we generated data with more complicated functions:

$$\begin{aligned} \eta(\mathbf{x}) &= \exp(x_3) - x_1 - x_2 - x_4 - x_5 & \mu(\mathbf{x}) &= 2 \times \mathbb{1}(x_2 + x_5 > 1) - x_3 \\ \mu_C(\mathbf{x}) &= x_1 x_3 - x_4 & \tau(\mathbf{x}) &= \sin(\pi x_1 x_2) - (x_3 - 0.5)^2 + .1x_4 - .2x_5. \end{aligned}$$

For each combination of $n \in \{500, 2000, 5000\}$ and $p \in \{5, 10, 25, 50, 75, 100\}$, we generated 100 synthetic datasets of size n . Figure 5 compares the performance of GRF to BCF-LATE as p and n increase. Like before, the gap between GRF and BCF-LATE diminishes as p increases while keeping n fixed and the gap increases somewhat as n increases while keeping p fixed; see Tables C3 and C4. Across nearly all combinations of n and p , BCF-LATE had smaller RMSE and interval score than GRF.

We conclude from our simulation studies that BCF-LATE is at least as capable as — and often better than — GRF in estimating the conditional local average treatment effects $\text{LATE}(\mathbf{x})$ in terms of point and interval estimation.

5 Results for Wellness Study

In this section, we apply BCF-LATE to public use data from the Illinois Workplace Wellness Study (Jones et al., 2019; Reif et al., 2020)¹. Of the 4,834 employees who joined the study, 1,534 were assigned to the control group while the other 3,300 were assigned to the treatment group and invited to participate in iThrive — the wellness program. Organizers offered financial awards to the treated subjects for completing the iThrive program and conducted multiple annual survey waves.

¹Data and codebooks available [here](#).

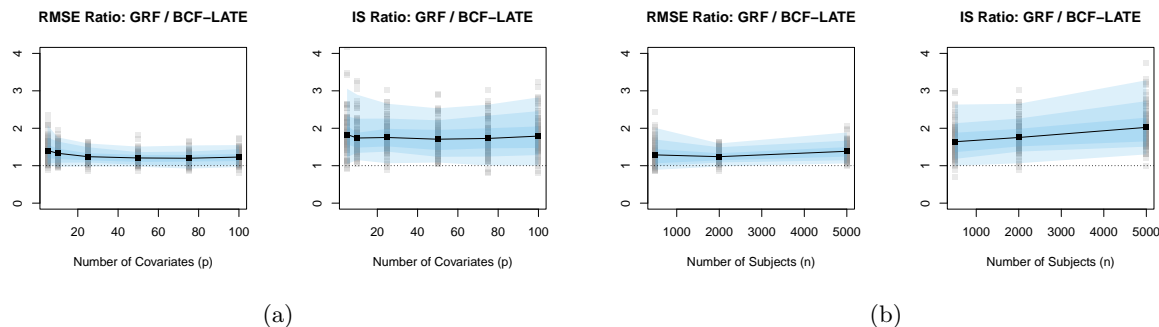


Figure 5: Comparison of BCF-LATE and GRF across 100 replications of the complex DGP when n is fixed and p increases (a) and when p is fixed and n increases (b). Each simulation is represented with a transparent gray square.

Our covariates, which were measured in the baseline survey administered in 2016, included demographics (e.g., age, race, sex); several health behavior and health history variables (e.g., smoking status and chronic conditions); and measures of job satisfaction. Except for age, which was discretized into “under 37”, “between 37 and 49”, and “over 49” years old, all covariates were binary. We focused on estimating the effect of participation in iThrive on three binary indicators measured in the 2017 follow-up survey: (i) whether subjects reported at least one chronic condition; (ii) whether subjects reported having high blood pressure, cholesterol, or blood glucose levels; and (iii) whether subjects believed that their health and safety was prioritized by their managers. See Tables D1 and D2 for summary statistics about all covariates and outcomes.

The public-use dataset also recorded whether subjects were invited to iThrive and whether they completed an online health risk assessment in 2016, which was required before they could participate in iThrive. Following Jones et al. (2019), we take completion of this assessment as a proxy for participation in the iThrive. Of the 3,330 subjects invited to iThrive, 1,848 completed the assessment. Hence, there are two important sources of variation to consider: natural variation generated from the random invitation to iThrive and variation in actual participation in iThrive. We defer additional information about how we preprocessed the data to Appendix D.

For each outcome, we ran four chains of BCF-LATE for 5,000 total iterations. After discarding the first half of each chain as “burn-in,” we obtained 10,000 MCMC draws of $\text{LATE}(\mathbf{x}_i)$ for each subject i . Figure 6 shows the distribution over the posterior mean $\text{LATE}(\mathbf{x}_i)$ ’s for each outcome. To better summarize the heterogeneity visible in these estimates, we fit a classification to predict the posterior mean estimates $\mathbb{E}[\text{LATE}(\mathbf{x}_i)|\mathbf{y}]$ using the covariates \mathbf{x}_i . Often called “fitting the fit,” this increasingly popular summarization step produces a parsimonious description of the conditional LATEs by splitting on covariates describing subgroups with the most meaningful heterogeneity (see, e.g., Hahn and Carvalho, 2015; Puelz et al., 2017; Fisher et al., 2020; Bolfarine et al., 2024). In other words, by fitting the fit, we can automatically identify interesting subgroups which may have significant positive or negative effects.

Self-report of chronic conditions. In Figure 6a, we observe a single prominent mode around a negative but negligible treatment effect (-0.0017). The summary tree in Figure 7a splits on covariates in symmetric positive and negative directions. It first splits on whether subjects rated their baseline health as very good or excellent: those that did are assigned to the right branch while those who did not are assigned to the left branch. Among those who did not rate their health as excellent or very good, iThrive participation decreased their chances of self-reporting a chronic condition in 2017 by 1.1 percentage points, on average. The far-left leaf node corresponds to a subgroup of white individuals who (i) did not rate their health as excellent or very good at baseline and (ii) did not report any chronic conditions at baseline. Within this subgroup, iThrive participation led to a 2.8 percentage point *decrease* in the changes of reporting at least one chronic health condition in 2017. In contrast, among non-white subjects who (i) rated their baseline health as excellent

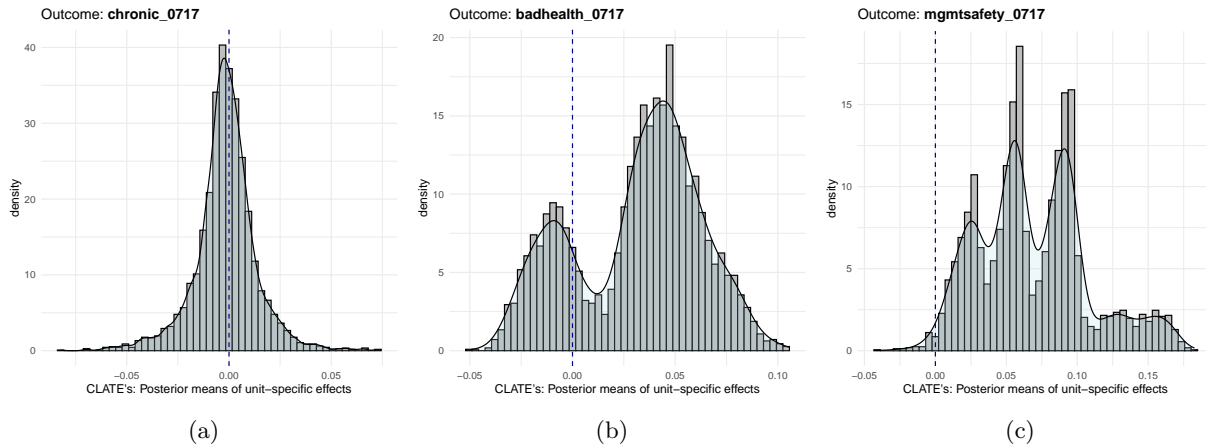


Figure 6: Distribution of the posterior means estimates of $LATE(x_i)$'s across our sample.

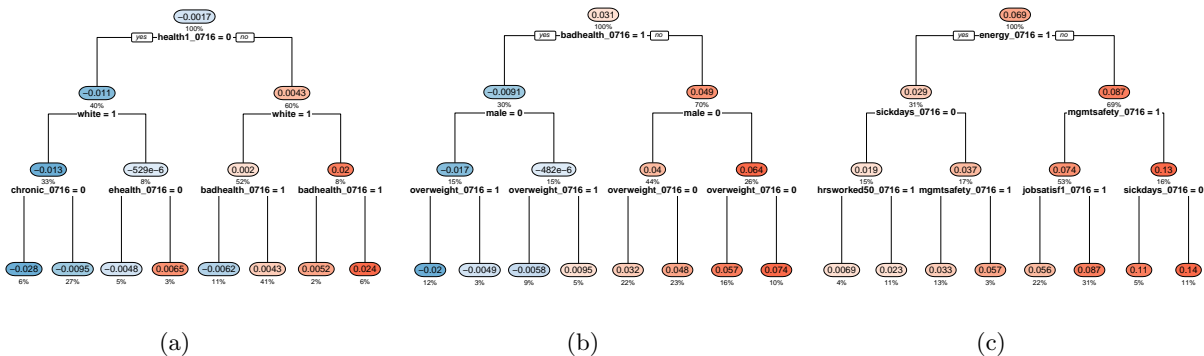


Figure 7: Trees summarizing the heterogeneity in fitted LATE estimates. Numbers within nodes are the subgroup average conditional LATE estimates. Nodes are colored according to the subgroup effect size, ranging from blue (for negative effect) to red (positive effect). Numbers below the nodes report the proportion of the sample in each subgroup.

or very good and (ii) did not report high blood pressure, cholesterol, or blood glucose at baseline (i.e., the far-right leaf in Figure 7a), iThrive participation led to a 2.4 percentage point *increase* in reporting at least one chronic health condition in 2017. Figure 8a shows the 90% posterior credible intervals for average effect within subgroup corresponding to the bottom nodes of Figure 7a. There is considerable posterior probability on both positive and negative effects within each subgroup and there is substantial overlap in the intervals across the subgroups. Consistent with Jones et al. (2019)'s findings, our results suggests that iThrive's impact on chronic conditions is essentially null and that there is not much heterogeneity in its effect.

Metabolic parameters. Figure 6b shows clear heterogeneity in the effect of iThrive participation on the chances that participants reported high cholesterol, blood pressure, or blood glucose (hereafter “metabolic parameters”) in 2017: there is a small mode around a small negative values and a more pronounced mode on moderate positive values. In fact, these two modes correspond to the first split in Figure 7b, which was on the variable `badhealth_0716`. This variable is equal to 1 if subjects self-reported high metabolic parameters at baseline in 2016 and is equal to 0 otherwise. The two modes in Figure 6b correspond to the subgroups formed by this first split: the positive mode aligns with those who said their cholesterol, blood pressure, and blood glucose levels were “low” or “normal” (Jones et al., 2019). These subjects were, in some sense, optimistic about their health status at baseline. Among these optimistic subjects, the posterior probability

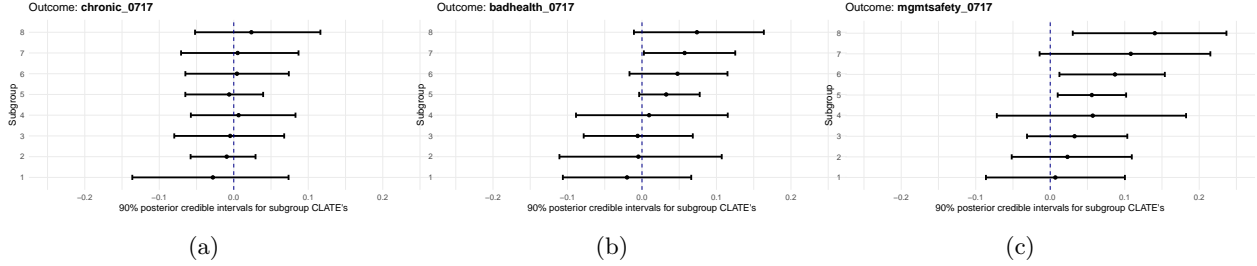


Figure 8: Credible intervals for the sample LATE within the subgroups corresponding to leaf nodes in the summary trees of Figure 7.

that the average effect of iThrive participation was positive was 92.4%. In sharp contrast, amongst subjects who were not optimistic about their baseline health, there is only a 42% posterior probability of a positive average effect of iThrive participation. The posterior distribution of the difference in the average effects across these subgroups placed about 93% probability on the positive axis. These results suggests that (i) the two modes visible in Figure 6b represent subgroups experiencing distinctly different effects of iThrive participation; and (ii) the dominant positive mode represents a real, non-zero treatment effect.

Our summary tree subdivides the optimistic subjects into four subgroups (the four rightmost leaves in Figure 7b and subgroups 5-8 in Figure 8b) based on their sex and whether they are considered overweight. The posterior distributions of the corresponding subgroup average effects place over 90% probability on positive values. The far-right leaf in the summary tree, the group with the highest chance of self-reporting high metabolic parameters in 2017, are those who were previously optimistic at baseline (first split), male (second split), and overweight at baseline (third split). iThrive participation elevated this subgroups chances of reporting high metabolic parameters by 7.4 percentage points.

At first glance, these findings appear counterintuitive at best and alarming at worst. There is, however, theoretical (Rosenstock et al., 1988) and empirical (Dalbo et al., 2017) psychological research supporting the divergence between health perception and reality. BCF-LATE identified a similar divergence in the Illinois Workplace Wellness Study data by uncovering the heterogeneity in this effect of iThrive participation.

Management’s prioritization of health & safety. Figure 6c displays a remarkable amount of heterogeneity with at least four well-defined modes. iThrive participation had a positive effect in each of the subgroups identified by the summary tree in Figure 7c. In fact, In Figure 8c the 90% credible intervals for the average effect in three out of the four subgroups in the right branch of the tree are entirely to the right of zero. This suggests that participating in iThrive increased the chances that subjects in these subgroups believed management prioritized their health and safety.

The summary tree splits on baseline sick days taken, overweight status, job satisfaction, and baseline belief that management prioritized employee well-being. The four different modes seen in Figure 6c line up with the four subgroups in the middle of the tree in Figure 7c (on the third row/after two splits). Among individuals who (i) did not self-report lots of energy at baseline; (ii) believe their managers prioritized their wellbeing at baseline (i.e., the far-right leaf in the third row of Figure 7c), iThrive participation increased the chances that they believed management prioritized their well-being by 13 percentage points. The posterior probability that this subgroup effect exceeded the other subgroup effects was 99%. This result is in line with the analysis in Jones et al. (2019), where they find a significant first-year treatment effect on the management prioritization outcome. BCF-LATE bolsters this finding by uncovering heterogeneity among the subjects’ effect sizes and showing which individuals within the sample drive this positive effect.

6 Discussion

In this paper we have proposed an extension of the Bayesian Causal Forest model (BCF) to account for one-sided noncompliance when outcomes of interest are binary. Our approach includes modeling compliance jointly with the outcome using nonlinear functions from Bayesian additive regression trees (BART [Chipman et al., 2010](#)). We have shown that by modeling compliance, our method performs better than traditional methods when compliance rates are low/the instrument is weak.

Using our method to analyze the Illinois Workplace Wellness Study ([Jones et al., 2019](#); [Reif et al., 2020](#)), we find that the conditional local average treatment effects vary for certain binary outcomes. Specifically, we find heterogeneity in the impact of the workplace wellness intervention on compliers’ rates of two self-reported health issues. Compliers who did not report high blood pressure, cholesterol, or glucose levels at baseline were more likely to report high metabolic parameter levels the following year if they were randomized to the wellness plan. Similarly, we find that while employees’ views about management’s priority on health and safety have a significant local average treatment effect like in [Jones et al. \(2019\)](#), we also see that there are subgroups of interest with varying magnitudes of effects.

Two future extensions are evident. First, our work here has been for one-sided noncompliance when the outcome is binary. Two-sided noncompliance introduces three or four latent strata, necessitating a multinomial model. [Chen et al. \(2024\)](#) and [Garraza et al. \(2024\)](#) both used a series of nested probit models to impute the latent strata. Rather than fitting multiple models, it would be interesting to use [Linero \(2024\)](#)’s generalized BART to model strata membership.

Second, Assumption [A1](#) implies that there is no interference across units. There may, however, be peer effects in which employees encourage each other to participate in iThrive. Estimating such peer effects is the subject of on-going work by the authors of [Jones et al. \(2019\)](#). It would be interesting to extend that work to explore treatment effect heterogeneity in the presence of interference.

Acknowledgements

We would like to thank Julian Reif, David Molitor, and Damon Jones for their advice with the data from their works ([Jones et al., 2019](#); [Reif et al., 2020](#)). We would also like to thank Jared Murray and Avi Feller for their ideas and support on the early variants of this project and Hyunseung Kang for several helpful discussions.

References

- Albert, J. H. and Chib, S. (1993). Bayesian analysis of binary and polychotomous response data. *Journal of the American Statistical Association*, 88(422):669–679.
- Andrews, I., Stock, J. H., and Sun, L. (2019). Weak instruments in instrumental variables regression: Theory and practice. *Annual Review of Economics*, 11(1):727–753.
- Angrist, J. D., Imbens, G. W., and Rubin, D. B. (1996). Identification of causal effects using instrumental variables. *Journal of the American Statistical Association*, 91(434):444–455.
- Angrist, J. D. and Pischke, J.-S. (2009). *Mostly harmless econometrics: An empiricist’s companion*. Princeton University Press.
- Athey, S., Tibshirani, J., and Wager, S. (2019). Generalized random forests. *Annals of Statistics*, 47(42):1148–1178.
- Athey, S. and Wager, S. (2019). Estimating treatment effects with causal forests: An application. *Observational Studies*, 5(2):37–51.
- Bargagli-Stoffi, F. J., De Witte, K., and Gnecco, G. (2022). Heterogeneous causal effects with imperfect compliance: A Bayesian machine learning approach. *The Annals of Applied Statistics*, 16(3):1986–2009.

- Bolfarine, H., Carvalho, C. M., Lopes, H. F., and Murray, J. S. (2024). Decoupling shrinkage and selection in gaussian linear factor analysis. *Bayesian Analysis*, 19(1):181–203.
- Chen, X., Harhay, M. O., Tong, G., and Li, F. (2024). A Bayesian machine learning approach for estimating heterogeneous survivor causal effects: Applications to a critical care trial. *The Annals of Applied Statistics*, 18(1):350–374.
- Chipman, H. A., George, E. I., and McCulloch, R. E. (1998). Bayesian CART model search. *Journal of the American Statistical Association*, 93(443):935–948.
- Chipman, H. A., George, E. I., and McCulloch, R. E. (2010). BART: Bayesian additive regression trees. *The Annals of Applied Statistics*, 4(1):266 – 298.
- Dalbo, V. J., Teramoto, M., Roberts, M. D., and Scanlan, A. T. (2017). Lack of reality: Positive self-perceptions of health in the presence of disease. *Sports*, 5(2):23.
- Deshpande, S. K., Bai, R., Balocchi, C., Starling, J. E., and Weiss, J. (2024). VCBART: Bayesian trees for varying coefficients. *arXiv preprint arXiv:2003.06416*.
- Fisher, J. D., Puelz, D. W., and Carvalho, C. M. (2020). Monotonic effects of characteristics on returns. *The Annals of Applied Statistics*, 14(4):1622 – 1650.
- Frangakis, C. E. and Rubin, D. B. (2002). Principal stratification in causal inference. *Biometrics*, 58(1):21–29.
- Garraza, L. G., Speizer, I., and Alkema, L. (2024). Combining BART and principal stratification to estimate the effect of intermediate on primary outcomes with application to estimating the effect of family planning on employment in Sub-Saharan Africa. *arXiv preprint arXiv:2408.03777*.
- Gneiting, T. and Raftery, A. E. (2007). Strictly proper scoring rules, prediction, and estimation. *Journal of the American Statistical Association*, 102(477):359–378.
- Hahn, P. R. and Carvalho, C. M. (2015). Decoupling shrinkage and selection in Bayesian linear models: A posterior summary perspective. *Journal of the American Statistical Association*, 110(509):435–448.
- Hahn, P. R., Murray, J. S., and Carvalho, C. M. (2020). Bayesian regression tree models for causal inference: Regularization, confounding, and heterogeneous effects (with discussion). *Bayesian Analysis*, 15(3):965–1056.
- Hill, J. L. (2011). Bayesian nonparametric modeling for causal inference. *Journal of Computational and Graphical Statistics*, 20(1):217–240.
- Imbens, G. W. and Rubin, D. B. (2015). *Causal inference in statistics, social, and biomedical sciences*. Cambridge University Press.
- Johnson, M., Cao, J., and Kang, H. (2022). Detecting heterogeneous treatment effects with instrumental variables and application to the Oregon health insurance experiment. *The Annals of Applied Statistics*, 16(2):1111–1129.
- Jones, D., Molitor, D., and Reif, J. (2019). What do workplace wellness programs do? evidence from the Illinois Workplace Wellness Study. *The Quarterly Journal of Economics*, 134(4):1747–1791.
- Kim, C. and Zigler, C. (2024). Bayesian nonparametric trees for principal causal effects. *arXiv preprint arXiv:2403.13256*.
- Künzel, S. R., Sekhon, J. S., Bickel, P. J., and Yu, B. (2019). Metalearners for estimating heterogeneous treatment effects using machine learning. *Proceedings of the National Academy of Sciences*, 116(10):4156–4165.
- Linero, A. R. (2018). Bayesian regression trees for high-dimensional prediction and variable selection. *Journal of the American Statistical Association*, 113(522):626–636.
- Linero, A. R. (2024). Generalized Bayesian additive regression trees models: Beyond conditional conjugacy. *Journal of the American Statistical Association*, pages 1–14.

- McCulloch, R. E., Sparapani, R. A., Logan, B. R., and Laud, P. W. (2021). Causal inference with the instrumental variable approach and bayesian nonparametric machine learning. *arXiv preprint arXiv:2102.01199*.
- Page, L. C., Feller, A., Grindal, T., Miratrix, L., and Somers, M.-A. (2015). Principal stratification: A tool for understanding variation in program effects across endogenous subgroups. *American Journal of Evaluation*, 36(4):514–531.
- Puelz, D., Hahn, P. R., and Carvalho, C. M. (2017). Variable selection in seemingly unrelated regressions with random predictors. *Bayesian Analysis*, 12(4):969–989.
- Ratkovic, M. and Shiraito, Y. (2014). Strengthening weak instruments by modeling compliance. In *Annual Meeting of the Midwest Political Science Association*.
- Reif, J., Chan, D., Jones, D., Payne, L., and Molitor, D. (2020). Effects of a workplace wellness program on employee health, health beliefs, and medical use: A randomized clinical trial. *JAMA Internal Medicine*, 180(7):952–960.
- Rosenstock, I. M., Strecher, V. J., and Becker, M. H. (1988). Social learning theory and the health belief model. *Health Education Quarterly*, 15(2):175–183.
- Wager, S. and Athey, S. (2018). Estimation and inference of heterogeneous treatment effects using random forests. *Journal of the American Statistical Association*, 113(523):1228–1242.
- Wald, A. (1940). The fitting of straight lines if both variables are subject to error. *The Annals of Mathematical Statistics*, 11(3):284–300.

A Constant LATE derivations

Recall that the constant local average treatment effect (LATE) is

$$\text{LATE} = \mathbb{E}[Y_i(1, 1) - Y_i(0, 0) | C_i = 1].$$

This notation is made possible by Assumptions [A1](#) and [A2](#).

A.1 Observables

To show the identification of the estimators in the paper, we begin by formalizing the observed values. Potential outcome notation is made possible by Assumption [A1](#).

$$\begin{aligned} R_i^{\text{obs}} &= A_i R_i(1) + (1 - A_i) R_i(0) \\ Y_i^{\text{obs}} &= A_i Y_i(1, R_i(1)) + (1 - A_i) Y_i(0, R_i(0)) \end{aligned}$$

With the latter assumptions, these can be simplified to other useful quantities.

First, note that the definition of complier via Assumption [A2](#) means $C_i = R_i(1)$, which confirms that complier-status is latent when $A_i = 0$. Combined with Assumption [A2](#), where $R_i(0) = 0$, we see that

$$R_i^{\text{obs}} = A_i C_i + (1 - A_i)(0) = A_i C_i. \quad (\text{A1})$$

Second, we note that $Y_i(1, R_i(1)) = C_i Y_i(1, 1) + (1 - C_i) Y_i(1, 0)$, such that Assumptions [A1](#) and [A2](#) also lead to

$$\begin{aligned} Y_i^{\text{obs}} &= A_i Y_i(1, R_i(1)) + (1 - A_i) Y_i(0, R_i(0)) \\ &= A_i [C_i Y_i(1, 1) + (1 - C_i) Y_i(1, 0)] + (1 - A_i) Y_i(0, R_i(0)) \\ &= A_i C_i Y_i(1, 1) + A_i (1 - C_i) Y_i(1, 0) + (1 - A_i) Y_i(0, 0) \end{aligned} \quad (\text{A2})$$

and, as such, it is simple to show that the three summands above point to the three quantities we can most easily estimate with observables:

$$\mathbb{E}[Y_i^{\text{obs}} | A_i = 1, C_i = 1] = \mathbb{E}[Y_i(1, 1) | A_i = 1, C_i = 1] \quad (\text{A3})$$

$$\mathbb{E}[Y_i^{\text{obs}} | A_i = 1, C_i = 0] = \mathbb{E}[Y_i(1, 0) | A_i = 1, C_i = 0] \quad (\text{A4})$$

$$\mathbb{E}[Y_i^{\text{obs}} | A_i = 0] = \mathbb{E}[Y_i(0, 0) | A_i = 0]. \quad (\text{A5})$$

With these preliminaries, we expand these statements with the next two assumptions. Assumption [A3](#) yields $Y_i(0, 0) = Y_i(1, 0)$, which changes Equation [A2](#) to

$$\begin{aligned} Y_i^{\text{obs}} &= A_i C_i Y_i(1, 1) + A_i (1 - C_i) Y_i(0, 0) + (1 - A_i) Y_i(0, 0) \\ &= A_i C_i Y_i(1, 1) + (1 - A_i C_i) Y_i(0, 0). \end{aligned} \quad (\text{A6})$$

Assumption [A3](#) also augments Equation [A4](#) into:

$$\mathbb{E}[Y_i^{\text{obs}} | A_i = 1, C_i = 0] = \mathbb{E}[Y_i(1, 0) | A_i = 1, C_i = 0] = \mathbb{E}[Y_i(0, 0) | A_i = 1, C_i = 0].$$

Assumption [A4](#) means many of the above equations hold without being conditioned on assignment A_i :

$$\begin{aligned} \mathbb{E}[Y_i(1, 1) | C_i = 1] &= \mathbb{E}[Y_i^{\text{obs}} | A_i = 1, C_i = 1] \\ \mathbb{E}[Y_i(1, 0) | C_i = 0] &= \mathbb{E}[Y_i^{\text{obs}} | A_i = 1, C_i = 0] \\ \mathbb{E}[Y_i(0, 0) | C_i = 0] &= \mathbb{E}[Y_i^{\text{obs}} | A_i = 1, C_i = 0] \\ \mathbb{E}[Y_i(0, 0)] &= \mathbb{E}[Y_i^{\text{obs}} | A_i = 0]. \end{aligned} \quad (\text{A7})$$

A.2 Identification of ITT_R

$$\begin{aligned}
\mathbb{E}[R_i^{\text{obs}}|A_i = 1] - \mathbb{E}[R_i^{\text{obs}}|A_i = 0] &= \mathbb{E}[A_i R_i(1) + (1 - A_i)R_i(0)|A_i = 1] \\
&\quad - \mathbb{E}[A_i R_i(1) + (1 - A_i)R_i(0)|A_i = 0] \\
&= \mathbb{E}[R_i(1)|A_i = 1] - \mathbb{E}[R_i(0)|A_i = 0] \\
&= \mathbb{E}[R_i(1)] - \mathbb{E}[R_i(0)] \\
&= \text{ITT}_R
\end{aligned}$$

A.3 Identification of ITT_Y

$$\begin{aligned}
\mathbb{E}[Y_i^{\text{obs}}|A_i = 1] - \mathbb{E}[Y_i^{\text{obs}}|A_i = 0] &= \mathbb{E}[A_i Y_i(1, R_i(1)) + (1 - A_i)Y_i(0, R_i(0))|A_i = 1] \\
&\quad - \mathbb{E}[A_i Y_i(1, R_i(1)) + (1 - A_i)Y_i(0, R_i(0))|A_i = 0] \\
&= \mathbb{E}[Y_i(1, R_i(1))|A_i = 1] - \mathbb{E}[A_i Y_i(1, R_i(1)) \\
&\quad + (1 - A_i)Y_i(0, R_i(0))|A_i = 0] \\
&= \mathbb{E}[Y_i(1, R_i(1))] - \mathbb{E}[Y_i(0, R_i(0))] \\
&= \text{ITT}_Y
\end{aligned}$$

A.4 The Wald Estimator

The standard estimator for the local average treatment effect for a binary instrument A_i is the Wald estimator (Wald, 1940), which is a ratio of the ITT_Y to ITT_R (Imbens and Rubin, 2015).

$$\frac{\text{ITT}_Y}{\text{ITT}_R} = \frac{\mathbb{E}[Y_i^{\text{obs}}|A_i = 1] - \mathbb{E}[Y_i^{\text{obs}}|A_i = 0]}{\mathbb{E}[R_i^{\text{obs}}|A_i = 1] - \mathbb{E}[R_i^{\text{obs}}|A_i = 0]} \tag{A8}$$

which we can show is equivalent to LATE using the previously Assumptions A1-A5. First note the following simplifications of the expectations in the denominator.

$$\begin{aligned}
\mathbb{E}[R_i^{\text{obs}}|A_i = 0] &= \mathbb{E}[A_i C_i|A_i = 0] = 0 \\
\mathbb{E}[R_i^{\text{obs}}|A_i = 1] &= \mathbb{E}[A_i C_i|A_i = 1] = \mathbb{E}[C_i|A_i = 1] = \mathbb{E}[C_i] = \mathbb{P}(C_i = 1) = \pi_C
\end{aligned} \tag{A9}$$

where the second line uses the fact that $C_i = R_i(1)$ and Assumption A4, i.e. $A_i \perp R_i(1)$, which together yield $A_i \perp C_i$. Thus, the compliance rate $\pi_C = \mathbb{P}(C_i = 1)$ is something we can identify.

Now for the numerator of Equation A8, we already have part of it from Equation A7, so the remaining component identifies the following:

$$\begin{aligned}
\mathbb{E}(Y_i^{\text{obs}}|A_i = 1) &= \mathbb{E}[A_i C_i Y_i(1, 1) + (1 - A_i C_i)Y_i(0, 0)|A_i = 1] \\
&= \mathbb{E}[C_i Y_i(1, 1) + (1 - C_i)Y_i(0, 0)|A_i = 1] \\
&= \mathbb{E}[C_i Y_i(1, 1) + (1 - C_i)Y_i(0, 0)] \\
&= \mathbb{P}(C_i = 0)\mathbb{E}[C_i Y_i(1, 1) + (1 - C_i)Y_i(0, 0)|C_i = 0] \\
&\quad + \mathbb{P}(C_i = 1)\mathbb{E}[C_i Y_i(1, 1) + (1 - C_i)Y_i(0, 0)|C_i = 1] \\
&= \mathbb{P}(C_i = 0)\mathbb{E}[Y_i(0, 0)|C_i = 0] + \mathbb{P}(C_i = 1)\mathbb{E}[Y_i(1, 1)|C_i = 1] \\
&= (1 - \pi_C)\mathbb{E}[Y_i(0, 0)|C_i = 0] + \pi_C\mathbb{E}[Y_i(1, 1)|C_i = 1]
\end{aligned}$$

Now, putting it all together:

$$\begin{aligned}
\frac{\text{ITT}_Y}{\text{ITT}_R} &= \frac{\mathbb{E}[Y_i^{\text{obs}}|A_i = 1] - \mathbb{E}[Y_i^{\text{obs}}|A_i = 0]}{\mathbb{E}[R_i^{\text{obs}}|A_i = 1] - \mathbb{E}[R_i^{\text{obs}}|A_i = 0]} \\
&= \frac{(1 - \pi_C)\mathbb{E}[Y_i(0,0)|C_i = 0] + \pi_C\mathbb{E}[Y_i(1,1)|C_i = 1] - \mathbb{E}[Y_i(0,0)]}{\pi_C - 0} \\
&= \mathbb{E}[Y_i(1,1)|C_i = 1] \\
&\quad + \frac{(1 - \pi_C)\mathbb{E}[Y_i(0,0)|C_i = 0] - (1 - \pi_C)\mathbb{E}[Y_i(0,0)|C_i = 0] - \pi_C\mathbb{E}[Y_i(0,0)|C_i = 1]}{\pi_C} \\
&= \mathbb{E}[Y_i(1,1)|C_i = 1] - \mathbb{E}[Y_i(0,0)|C_i = 1] \\
&= \text{LATE}.
\end{aligned}$$

B Gibbs sampler derivation

To derive our Gibbs sampler, we introduce some additional notation. Given a regression tree (T, \mathcal{B}) and a point \mathbf{x} , let $\ell(\mathbf{x}; T)$ be the leaf of T associated with \mathbf{x} . Further, let $g(\mathbf{x}; T, \mathcal{B})$ be the evaluation function that returns the jump associated with $\ell(\mathbf{x}; T)$; that is

$$g(\mathbf{x}; T, \mathcal{B}) = \beta_{\ell(\mathbf{x}; T)}.$$

With this notation, we can write

$$\mu(\mathbf{x}) = \sum_{m=1}^{M_\mu} g(\mathbf{x}; T_m^{(\mu)}, \mathcal{B}_m^{(\mu)}).$$

We can analogously express each of $\mu_c(\mathbf{x})$, $\tau(\mathbf{x})$, and $\eta(\mathbf{x})$ as sums of tree evaluations. Finally, let $\Theta = \{\theta^{(\mu)}, \theta^{\mu_c}, \theta^{(\tau)}, \theta^{(\eta)}\}$ denote the collection of prior variable splitting probabilities.

B.1 Sampling latent utilities and missing compliance statuses

Each iteration of our Gibbs sampler begins by first sampling the missing compliance statuses $\mathbf{C}^{(0)}$ and then drawing latent utilities \tilde{Y}_i and \tilde{C}_i for each subject.

The joint conditional density of unobserved compliance statuses for control subjects is given by

$$\begin{aligned}
p(\mathbf{C}^{(0)}|\mathbf{Y}, \mathcal{E}) &\propto \prod_{i:a_i=0} \left\{ [\Phi(\mu(\mathbf{x}_i) + \mu_c(\mathbf{x}_i) \times c_i)]^{y_i} \times [1 - \Phi(\mu(\mathbf{x}) + c_i \times \mu_c(\mathbf{x}))]^{1-y_i} \right\} \\
&\quad \times \prod_{i:a_i=0} \left\{ \Phi(\eta(\mathbf{x}))^{c_i} \times [1 - \Phi(\eta(\mathbf{x}_i))]^{1-c_i} \right\}.
\end{aligned} \tag{B1}$$

From (B1) we can conclude that the latent compliance statuses are conditionally independent given \mathcal{E} (which determines the functions μ , μ_c , τ , and η) and the observed outcomes \mathbf{Y} . We further compute

$$\begin{aligned}
\mathbb{P}(C_i = 1|Y_i = 1, \mathcal{E}) &= \frac{\Phi(\eta(\mathbf{x})) \times \Phi(\mu(\mathbf{x}_i) + \mu_c(\mathbf{x}_i))}{\Phi(\eta(\mathbf{x})) \times \Phi(\mu(\mathbf{x}_i) + \mu_c(\mathbf{x}_i)) + (1 - \Phi(\eta(\mathbf{x}))) \times \Phi(\mu(\mathbf{x}_i))} \\
\mathbb{P}(C_i = 1|Y_i = 0, \mathcal{E}) &= \frac{\Phi(\eta(\mathbf{x})) \times (1 - \Phi(\mu(\mathbf{x}_i) + \mu_c(\mathbf{x}_i)))}{\Phi(\eta(\mathbf{x})) \times (1 - \Phi(\mu(\mathbf{x}_i) + \mu_c(\mathbf{x}_i))) + (1 - \Phi(\eta(\mathbf{x}))) \times (1 - \Phi(\mu(\mathbf{x}_i)))}
\end{aligned} \tag{B2}$$

So, in the first step of each Gibbs sampling iteration, we sample a new value of $\mathbf{C}^{(0)}$ by independently drawing C_i 's according to Equation (B2).

Having drawn the missing compliance statuses, our data likelihood is now

$$p(\mathbf{Y}, \mathbf{C} | \mathcal{E}) \propto \prod_{i=1}^n \left[\Phi(f(\mathbf{x}_i, c_i, a_i))^{y_i} \times (1 - \Phi(f(\mathbf{x}_i, c_i, a_i)))^{1-y_i} \times \Phi(\eta(\mathbf{x}_i))^{c_i} \times (1 - \Phi(\eta(\mathbf{x}_i)))^{1-c_i} \right].$$

Following [Albert and Chib \(1993\)](#), we introduce latent utilities \tilde{Y}_i and \tilde{C}_i such that $Y_i = \mathbb{1}(\tilde{Y}_i \geq 0)$ and $C_i = \mathbb{1}(\tilde{C}_i \geq 0)$, yielding the augmented likelihood

$$\begin{aligned} p(\mathbf{Y}, \mathbf{C}, \tilde{\mathbf{Y}}, \tilde{\mathbf{C}} | \mathcal{E}) &\propto \exp \left\{ -\frac{1}{2} \sum_{i=1}^n (\tilde{y}_i - f(\mathbf{x}_i, c_i, a_i))^2 \right\} \times \prod_{i=1}^n \mathbb{1} \left(Y_i = \mathbb{1}(\tilde{Y}_i \geq 0) \right) \\ &\times \exp \left\{ -\frac{1}{2} \sum_{i=1}^n (\tilde{c}_i - \eta(\mathbf{x}_i))^2 \right\} \times \prod_{i=1}^n \mathbb{1} \left(C_i = \mathbb{1}(\tilde{C}_i \geq 0) \right). \end{aligned} \quad (\text{B3})$$

From Equation (B3), we conclude that

$$\tilde{Y}_i \sim \mathbb{1}(Y_i = 1) \times \mathcal{N}_+(f(\mathbf{x}_i, c_i, a_i), 1) + \mathbb{1}(Y_i = 0) \times \mathcal{N}_-(f(\mathbf{x}_i, c_i, a_i), 1) \quad (\text{B4})$$

$$\tilde{C}_i \sim \mathbb{1}(C_i = 1) \times \mathcal{N}_+(\eta(\mathbf{x}_i), 1) + \mathbb{1}(C_i = 0) \times \mathcal{N}_-(\eta(\mathbf{x}_i), 1), \quad (\text{B5})$$

where \mathcal{N}_+ and \mathcal{N}_- respectively denote truncations of a normal distribution to the positive and negative axes. The second step of each Gibbs sampling iteration begins by drawing latent utilities \tilde{Y}_i and \tilde{C}_i for each $i = 1, \dots, n$ according to Equations (B4) and (B5).

B.2 Updating regression trees

Once we draw the latent utilities $\tilde{\mathbf{Y}}$ and $\tilde{\mathbf{C}}$, we sweep over the trees in \mathcal{E} , updating them one at a time conditionally on the fits of all other trees and the latent variables. Each update involves sampling a regression tree (T, \mathcal{B}) from a particular conditional distribution whose density is of the form

$$p(T, \mathcal{B} | \tilde{\mathbf{Y}}, \tilde{\mathbf{C}}, \mathcal{E}^-) \propto p(T) p(\mathcal{B} | T) p(\tilde{\mathbf{Y}}, \tilde{\mathbf{C}} | T, \mathcal{B}, \mathcal{E}^-), \quad (\text{B6})$$

where \mathcal{E}^- denotes the collection of all other regression trees. We draw trees from such distributions in two steps. First, we sample the decision tree T from the corresponding marginal distribution. This is done using a variant of the Metropolis-Hastings approach introduced by [Chipman et al. \(1998\)](#) that only implements grow and prune moves. Then we sample $\mathcal{B} | T$ from its corresponding conditional.

From Equation (B3), that the ‘‘likelihood’’ term $p(\tilde{\mathbf{Y}}, \tilde{\mathbf{C}} | T, \mathcal{B}, \mathcal{E}^-)$ depends on $\tilde{\mathbf{Y}}$ and $\tilde{\mathbf{C}}$ through the *full residuals*

$$\begin{aligned} R_i^{(y)} &= \tilde{y}_i - f(\mathbf{x}_i, c_i, a_i) \\ R_i^{(c)} &= \tilde{c}_i - \eta(\mathbf{x}_i). \end{aligned}$$

Updating $\mathcal{E}^{(\mu)}$. To update the m -th tree $(T_m^{(\mu)}, \mathcal{B}_m^{(\mu)})$ in $\mathcal{E}^{(\mu)}$, we set

$$p(\tilde{\mathbf{Y}}, \tilde{\mathbf{C}} | T, \mathcal{B}, \mathcal{E}^-) = \exp \left\{ -\frac{1}{2} \left[\sum_{i=1}^n (r_i^{(\mu)} - g(\mathbf{x}_i; T, \mathcal{B}))^2 \right] \right\}, \quad (\text{B7})$$

where $r_i^{(\mu)}$ is the partial residual

$$r_i^{(\mu)} = R_i^{(y)} + g(\mathbf{x}_i; T_m^{(\mu)}, \mathcal{B}_m^{(\mu)}). \quad (\text{B8})$$

Updating $\mathcal{E}^{(\mu_c)}$. To update the m -th tree $(T_m^{(\mu_c)}, \mathcal{B}_m^{(\mu_c)})$ in $\mathcal{E}^{(\mu_c)}$, we set

$$p(\tilde{\mathbf{Y}}, \tilde{\mathbf{C}}|T, \mathcal{B}, \mathcal{E}^-) = \exp \left\{ -\frac{1}{2} \left[\sum_{i=1}^n (r_i^{(\mu_c)} - c_i \times g(\mathbf{x}_i; T, \mathcal{B}))^2 \right] \right\}. \quad (\text{B9})$$

introduce the partial residual

$$r_i^{(\mu_c)} = R_i^{(y)} + c_i \times g(\mathbf{x}_i; T, \mathcal{B}). \quad (\text{B10})$$

Then the conditional posterior density of the m -th tree is

Updating $\mathcal{E}^{(\tau)}$. To update the m -th tree $(T_m^{(\tau)}, \mathcal{B}_m^{(\tau)})$ in $\mathcal{E}^{(\tau)}$, we introduce the partial residual

$$r_i^{(\tau)} = R_i^{(y)} + c_i \times a_i \times g(\mathbf{x}_i; T, \mathcal{B}) \quad (\text{B11})$$

Then the conditional posterior density of the m -th tree is

$$p(\tilde{\mathbf{Y}}, \tilde{\mathbf{C}}|T, \mathcal{B}, \mathcal{E}^-) = \exp \left\{ -\frac{1}{2} \left[\sum_{i=1}^n (r_i^{(\tau)} - c_i \times a_i \times g(\mathbf{x}_i; T, \mathcal{B}))^2 \right] \right\}. \quad (\text{B12})$$

Updating $\mathcal{E}^{(\eta)}$. To update the m -th tree $(T_m^{(\eta)}, \mathcal{B}_m^{(\eta)})$ in $\mathcal{E}^{(\eta)}$, we set

$$p(\tilde{\mathbf{Y}}, \tilde{\mathbf{C}}|T, \mathcal{B}, \mathcal{E}^-) = \exp \left\{ -\frac{1}{2} \sum_{i=1}^n \left(r_i^{(\eta)} - g(\mathbf{x}_i; T, \mathcal{B}) \right)^2 \right\}, \quad (\text{B13})$$

where

$$r_i^{(\eta)} = R_i^{(c)} + g(\mathbf{x}_i; T, \mathcal{B}). \quad (\text{B14})$$

B.3 Updating splitting probabilities

Once we update each tree in \mathcal{E} , we update the elements of Θ conditionally on ξ and then update each element of ξ , conditionally on Θ . Update $\theta^{(\mu)}|\xi^{(\mu)}$ involves nothing more than a Dirichlet-Multinomial update. To update $\xi^{(\mu)}|\theta^{(\mu)}$, we use the Metropolis algorithm where proposals are drawn from the Beta(0.5, 1) prior on $\xi^{(\mu)}/(\xi^{(\mu)} + p)$. We similarly update the other components of Θ and ξ .

C Additional simulation results

Table C1: LATE(\mathbf{x}) estimation performance for BCF-LATE and GRF on simple DGP. Metrics are averages for the 100 simulations, with n=2000. Coverage is 95% interval coverage. IS is the interval score of [Gneiting and Raftery \(2007\)](#), where smaller scores indicate better interval prediction. Ratios use BCF-LATE as a baseline, such that values greater than one indicate BCF-LATE performed better than GRF on average.

p	BCF-LATE				GRF				Ratio: GRF/BCF-LATE	
	RMSE	Coverage	Width	IS	RMSE	Coverage	Width	IS	RMSE	IS
2	0.115	0.883	0.352	0.018	0.797	0.955	2.503	0.066	6.965	3.765
5	0.110	0.901	0.356	0.017	0.455	0.955	1.678	0.045	4.181	2.714
10	0.108	0.910	0.367	0.016	0.355	0.966	1.665	0.043	3.326	2.706
25	0.103	0.924	0.385	0.016	0.273	0.977	1.469	0.038	2.673	2.392
50	0.101	0.931	0.405	0.016	0.164	0.933	0.897	0.026	1.629	1.634
75	0.102	0.930	0.404	0.016	0.177	0.836	0.727	0.027	1.740	1.701
100	0.116	0.926	0.452	0.017	0.213	0.730	0.704	0.035	1.915	2.086

Table C2: LATE(\mathbf{x}) estimation performance for BCF-LATE and GRF on a simple data-generating process. Metrics are averages for the 100 simulations, with $p = 25$. Coverage is 95% interval coverage, and ideally is 0.95. IS is the interval score of [Gneiting and Raftery \(2007\)](#), where smaller scores indicate better interval prediction. Ratios use BCF-LATE as a baseline, such that values greater than one indicate BCF-LATE performed better than GRF on average.

n	BCF-LATE				GRF				Ratio: GRF/BCF-LATE	
	RMSE	Coverage	Width	IS	RMSE	Coverage	Width	IS	RMSE	IS
500	0.210	0.730	0.447	0.037	0.337	0.886	1.535	0.048	1.616	1.332
2000	0.103	0.924	0.385	0.016	0.273	0.977	1.469	0.038	2.673	2.392
5000	0.069	0.965	0.326	0.011	0.350	0.989	1.752	0.044	5.076	4.161

Table C3: LATE(\mathbf{x}) estimation performance for BCF-LATE and GRF on a challenging data-generating process. Metrics are averages for 100 simulations, with $n=2000$ and only five covariates involved in the DGP. Coverage is 95% interval coverage, and ideally is 0.95. IS is the interval score of [Gneiting and Raftery \(2007\)](#), where smaller scores indicate better interval prediction. Ratios use BCF-LATE as a baseline, such that values greater than one indicate BCF-LATE performed better than GRF on average.

p	BCF-LATE				GRF				Ratio: GRF/BCF-LATE	
	RMSE	Coverage	Width	IS	RMSE	Coverage	Width	IS	RMSE	IS
5	0.084	0.922	0.294	0.010	0.116	0.875	0.418	0.018	1.405	1.833
10	0.087	0.919	0.305	0.010	0.114	0.935	0.554	0.017	1.332	1.739
25	0.091	0.920	0.321	0.011	0.112	0.943	0.594	0.018	1.241	1.754
50	0.093	0.921	0.329	0.011	0.111	0.939	0.579	0.018	1.207	1.707
75	0.094	0.921	0.333	0.011	0.111	0.945	0.611	0.019	1.199	1.728
100	0.094	0.929	0.339	0.011	0.114	0.949	0.650	0.019	1.230	1.791

Table C4: LATE(\mathbf{x}) estimation performance for BCF-LATE and GRF on a challenging data-generating process. Metrics are averages for the 100 simulations, with $p = 25$ but only five covariates involved in the DGP. Coverage is 95% interval coverage, and ideally is 0.95. IS is the interval score of [Gneiting and Raftery \(2007\)](#), where smaller scores indicate better interval prediction. Ratios use BCF-LATE as a baseline, such that values greater than one indicate BCF-LATE performed better than GRF on average.

n	BCF-LATE				GRF				Ratio: GRF/BCF-LATE	
	RMSE	Coverage	Width	IS	RMSE	Coverage	Width	IS	RMSE	IS
500	0.106	0.922	0.395	0.013	0.135	0.946	0.707	0.021	1.289	1.640
2000	0.091	0.920	0.321	0.011	0.112	0.943	0.594	0.018	1.241	1.754
5000	0.074	0.932	0.267	0.009	0.101	0.953	0.572	0.017	1.385	2.024

D Background on the Illinois Workplace Wellness Study

Table D1: Variable names and summary statistics for the **covariates** considered. These are the baseline survey values obtained in 2016. The second column is the number of non-missing observations, the third through fifth are sample statistics, and the final column is a description extracted from the survey data codebook. The mean statistics represent the average number of “1’s” across available observations since all outcomes are binary variables except for the “age” covariate.

Covariates	N	Mean	Min	Max	Description
male	4834	0.43	0	1	Male indicator
age	4834	0.99	0	2	0 = less than 37, 1 = 37-49, 2 = greater than 49
white	4834	0.84	0	1	White race indicator
everscreen_0716	4834	0.89	0	1	Had at least 1 previous health screening (2016)
active_0716	4834	0.37	0	1	Physically active (2016)
active_try_0716	4834	0.81	0	1	Trying to be more active (2016)
cursmk_0716	4833	0.07	0	1	Current smoker (2016)
othersmk_0716	4833	0.09	0	1	Other (non-cigarette) tobacco use (2016)
formsmk_0716	4833	0.20	0	1	Former smoker (2016)
drink_0716	4830	0.65	0	1	Drinker (2016)
drinkhvy_0716	4829	0.05	0	1	Heavy drinker (2016)
chronic_0716	4834	0.73	0	1	Has at least 1 chronic condition (2016)
health1_0716	4834	0.60	0	1	Health is excellent or very good (2016)
health2_0716	4834	0.99	0	1	Health is not poor (2016)
problems_0716	4834	0.39	0	1	Problems with physical activities or pain (2016)
energy_0716	4834	0.32	0	1	Lots of energy (2016)
ehealth_0716	4834	0.29	0	1	Emotional health (2016)
overweight_0716	4834	0.54	0	1	Overweight status (2016)
badhealth_0716	4834	0.30	0	1	High blood pressure, cholesterol, or glucose (2016)
sedentary_0716	4833	0.54	0	1	Sedentary job (2016)
druguse_0716	4830	0.71	0	1	Taking 1+ prescription/OTC drugs (2016)
physician_0716	4833	0.76	0	1	Physician or ER utilization (2016)
hospital_0716	4833	0.03	0	1	Hospital utilization (2016)
sickdays_0716	4828	0.61	0	1	Sick days in past 12 months (baseline survey) (2016)
hrsworked50_0716	4831	0.18	0	1	Worked 50 or more hours per week (2016)
jobsatisf1_0716	4832	0.40	0	1	Very satisfied with job (2016)
jobsatisf2_0716	4832	0.84	0	1	Very or somewhat satisfied with job (2016)
mgmtsafety_0716	4831	0.78	0	1	Management places very high or some priority on health/safety (2016)

Table D2: Variable names and summary statistics for the **outcomes** considered. The second column is the number of non-missing observations, the third through fifth are sample statistics, and the final column is a description extracted from the survey data codebook. All outcomes have missing observations since the sample sizes are less than the entire experimental group of 4,834. The mean statistics represent the average number of “1’s” across available observations since all outcomes are binary variables.

Outcomes	N	Mean	Min	Max	Description
chronic_0717	3565	0.73	0	1	Has at least 1 chronic condition (2017)
badhealth_0717	3567	0.32	0	1	High blood pressure, cholesterol, or glucose (2017)
mgmtsafety_0717	3566	0.79	0	1	Management places very high or some priority on health/safety (2017)